The low-temperature thermal history of northern Switzerland as revealed by fission track analysis and inverse thermal modelling

Zoltan Timar-Geng[1*], Bernhard Fügenschuh[1**], Andreas Wetzel[1] & Horst Dresmann[1]

ABSTRACT

New zircon and apatite fission track (FT) data from four boreholes, which penetrate the Mesozoic and pre-Mesozoic sediments and crystalline basement of northern Switzerland, are presented. Inverse thermal modelling of the measured apatite FT parameters unravels the low-temperature (below ~120 °C) thermal history of the crystalline basement of northern Switzerland. Zircon FT central and single-grain ages cluster around 250 Ma, thus maximum palaeotemperatures did not exceed ~330 °C after late-Variscan consolidation of the crystalline basement. Apatite FT central ages vary between 25 and 87 Ma. Confined mean track lengths range between 9.3 µm and 11.6 µm, suggesting substantial track annealing within all apatite samples. Modelled time-temperature paths offer a clear picture about the low-temperature thermal history of the crystalline basement of northern Switzerland: Cretaceous cooling is followed by an Eocene heating event and subsequent cooling to present-day temperatures. The Eocene heating episode is contemporaneous with the initial rifting stage of the nearby Upper Rhine Graben and the associated increasing volcanic activity. Crustal-scale faults of the Permo-Carboniferous Trough of northern Switzerland could have acted as major pathways for circulating hydrothermal fluids giving rise to the observed Middle to Late Eocene thermal event.

ZUSAMMENFASSUNG

Neue Zirkon- und Apatit-Spaltspurdaten werden aus vier Bohrungen, welche die mesozoische und pre-mesozoische Sedimentbedeckung, sowie das oberste kristalline Grundgebirge der Nordschweiz durchteufen, vorgelegt. Inverse thermische Modellierung der gemessenen Apatit-Spaltspurparameter erlaubt, die Niedrigtemperaturgeschichte (unter ~120 °C) des kristallinen Grundgebirges der Nordschweiz zu enträtseln. Die Zirkon-Spaltspuralter (Zentralalter) und die Einzelkornalter zeigen eine Häufung um 250 Ma. Daraus folgt, dass die maximalen Paläotemperaturen nach der spätvariszischen Konsolidierung des Kristallins ~330 °C nicht mehr überschritten haben. Apatit-Spaltspuralter (Zentralalter) variieren zwischen 25 und 87 Ma. Die mittleren Spaltspurlängen reichen von 9,3 µm bis 11,6 µm und weisen auf eine substantielle Ausheilung in den Apatiten hin. Die modellierten Zeit-Temperatur-Pfade bieten ein klares Bild der Niedrigtemperaturgeschichte des kristallinen Grundgebirges in der Nordschweiz: Einer kretazischen Abkühlung folgt ein eozänes Wärmeereignis und anschliessend eine Abkühlung zur heutigen Temperaturverteilung. Der eozäne Wärmepuls ist zeitgleich mit der initialen Riftingphase des nahegelegenen Oberrheingrabens und der damit verbundenen erhöhten vulkanischen Aktivität. Zum Nordschweizer Permokarbontrog-System gehörige Störungen im Krustenmassstab könnten als Fliesswege für zirkulierende Fluide gedient haben, die zum beobachteten mittel- bis späteozänen thermischen Ereignis führten.

1. Introduction

The trend and the shape of fission track (FT) age-depth (or age-elevation) profiles provide important constraints on the thermal history of crustal segments. Most commonly ages decrease with depth. In a typical foreland basin, however, detrital FT ages might record the erosion history of the hinterland (e.g., Cederbom et al. 2004), and in some rare cases FT ages represent formation ages of, for example, volcanic ashes and, hence, are consistent with the chronostratigraphy (e.g., Naeser et al. 1987). The age-depth graphs vary from nearly linear in active orogenic belts to concave-upwards in cratonic regions with extremely low cooling rates, or alternatively, in sedimentary basins with slow heating due to progressive burial (e.g., Gleadow & Brown 2000). Significant acceleration of the cooling rate after a period of relative stability leads to a compound profile with a typical "break in slope", interpreted as the onset of rapid cooling (e.g., Gleadow & Brown 2000). Moreover, vertical sections are very convenient, when time-temperature paths experienced by individual samples are modelled, because the palaeogeothermal gradient at different times can be indirectly determined. Thus, the information from a vertical

[1]Geologisch-Paläontologisches Institut, Universität Basel, Bernoullistrasse 32, CH-4056 Basel, Switzerland.
*Present address: Geologisches Institut, Albert-Ludwigs-Universität Freiburg, Albertstr. 23b, D-79104 Freiburg, Germany.
E-mail: zoltan.timar-geng@geologie.uni-freiburg.de
**Present address: Institut für Geologie und Paläontologie, Universität Innsbruck, Innrain 52, A-6020 Innsbruck, Austria.
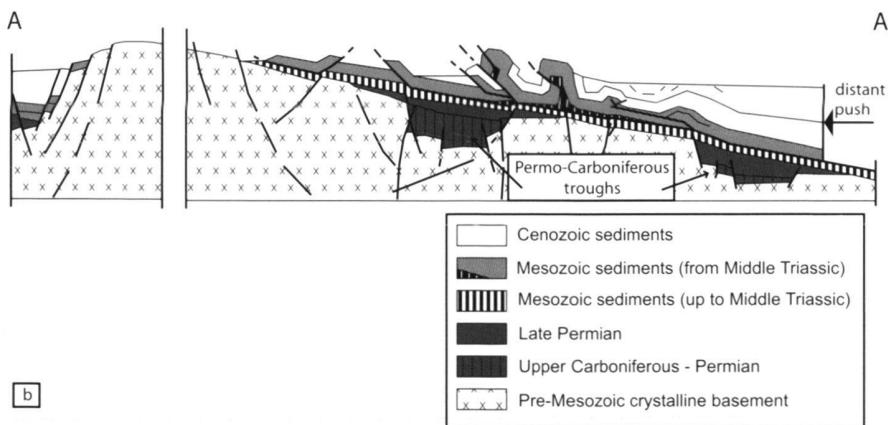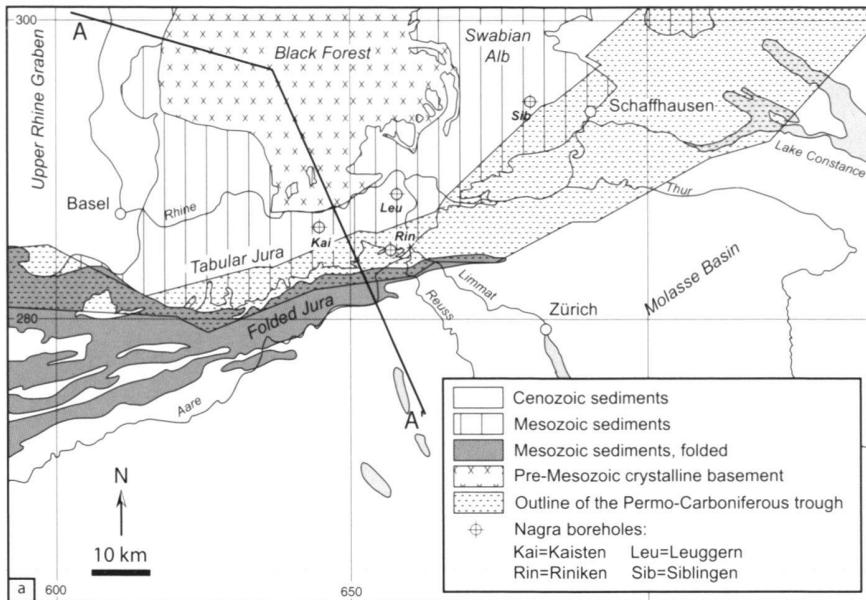
Fig. 1. (a) Tectonic sketch map and (b) schematic profile of the study area (after Thury et al. 1994).

alignment of samples is markedly better than that from any individual sample alone, provided that the samples did not experience tectonic displacements relative to each other during or after their recorded thermal histories. In regions with relatively low relief vertically aligned samples from deep boreholes are particularly favourable, since approximations to a true vertical section are possible only in mountainous regions with high relief. This sampling approach has led to many successful applications of FT analysis on borehole cores evaluating the thermal history of sedimentary basins (e.g., Gleadow et al. 1983; Green et al. 1989; Duddy 1994; Tingate & Duddy 2002; House et al. 2002) or revealing the palaeothermal anomalies in different geological settings (Green et al. 2001; Murakami et al. 2002).

Due to the lack of substantial relief in northern Switzerland, the analysis of borehole samples, in addition to surface

samples, is essential for a sound determination of the thermal history of the region.

In the course of an extensive geological investigation program for the assessment of the feasibility and safety of a repository for radioactive waste, Nagra (Swiss National Cooperative for the Disposal of Radioactive Waste) carried out several drillings in central northern Switzerland. Results are summarised in a number of reviews (e.g., Thury et al. 1994; Müller et al. 2002; Nagra 2002). In addition, the burial and the associated thermal history of the Molasse basin have been investigated by, for instance, Schegg & Leu (1998), and Nagra (2002). Applying a 1D basin modelling approach, Nagra (2002) postulated two heating events for the crystalline basement and the Mesozoic cover, a first one during the Early Cretaceous and a second one in the Late Miocene. These heating events are supported by available apatite FT modelling results (Mazurek et al. 2006).

This paper presents new zircon and apatite FT data from four of the Nagra boreholes (Fig. 1) and uses these data as input parameters for modelling the time-temperature paths experienced by the samples. The focus lies on the pre-Mesozoic crystalline basement and the Permo-Carboniferous Trough of northern Switzerland. The differences between the new results and the previous FT modelling results related to the thermal history of the Molasse basin (Mazurek et al. 2006) are also discussed. Finally, also the relationship to the FT results from the adjacent Upper Rhine Graben area (Timar-Geng et al. 2004; 2006) is investigated. This article provides new insights into the low-temperature thermal history of northern Switzerland and makes an important contribution to the assessment of safe disposal of radioactive waste in northern Switzerland.

2. Geological setting

Five main tectonic units are distinguished in northern Switzerland and adjacent SW Germany (Fig. 1): a) the crystalline basement, exposed in the Black Forest; b) the Permo-Carboniferous Trough of northern Switzerland which is not exposed at the surface; c) the autochtonous sedimentary cover of the Tabular Jura and the Swabian Alb; d) the sheared-off sedimentary cover comprising the Folded Jura and the Molasse Basin, and e) the Tertiary rift sediments of the Upper Rhine Graben.

The Late Palaeozoic consolidation of the crystalline basement of northern Switzerland was preceded by extensive Variscan deformation and metamorphism, accompanied by substantial magmatic activity, and the formation of the Permo-Carboniferous Trough of northern Switzerland (for details see overviews by, e.g., Thury et al. 1994; Müller et al. 2002). Well-stratified Triassic to Jurassic deposits accumulated in a shallow epicontinental sea and indicate relative tectonic stability. However, episodic reactivation of pre-existing basement structures during the Jurassic led to differential subsidence and synsedimentary deformation, documented by changes of facies and sediment thickness (Wetzel et al. 2003). Reactivated faults also acted as major conduits for hot fluids in the crystalline basement, as documented by Jurassic hydrothermal mineralisations, exposed, for example, in the nearby Black Forest and Vosges (for a compilation, see Wetzel et al. 2003). Mesozoic heating is also evidenced by palaeomagnetic data from the Vosges (Edel 1997), documenting post-Permian thermal overprinting. FT data from the southern Upper Rhine Graben area indicate that the Jurassic hydrothermal fluid migration affected the upper crust on a regional scale (Timar-Geng et al. 2004, 2006). Thus, it is very likely that substantial heating also occurred in the crystalline basement of northern Switzerland. A significant stratigraphic gap between the Upper Jurassic and middle Eocene deposits provides evidence of Cretaceous to early Tertiary erosion. However, it is still a matter of debate, how much Cretaceous sediments were deposited and subsequently eroded (e.g. Ziegler 1990).
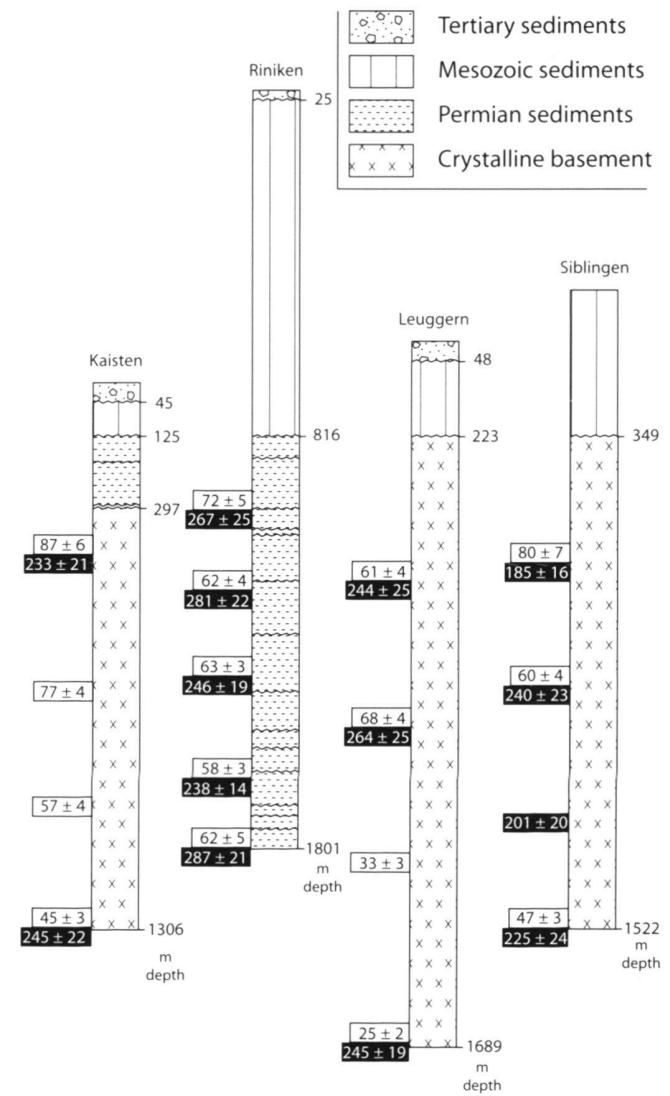
Fig. 2. Stratigraphic overview of the Nagra boreholes with zircon (in white letter on black background) and apatite FT central ages (black letter on white background). All ages are given with their 1σ error. The boreholes are leveled according to their common Mesozoic base unconformity. Waved horizontal lines indicate unconformities.

The Tertiary geological history of northern Switzerland and adjacent areas is a period of renewed tectonic activity, mainly related to Alpine orogeny. It includes the Eo-Oligocene subsidence of the Upper Rhine Graben, the subsequent updoming of the southern Black Forest, the subsidence of the Alpine foreland from the Late Oligocene onwards, and finally, the Late Miocene formation of the Jura Mountains. Ongoing tectonic activity is clearly documented for northern Switzerland and the southern Upper Rhine Graben area by the well-known increased seismicity (several strong earthquakes in historical times; see compilation by Müller et al.

Table 1. Sample details and present temperatures according to Nagra (1990; 1991a; 1991b; 1993).

Borehole	Sample No.	Depth (m)	Lithostratigraphy	Present temp. (°C)
Kaisten	Kai1	1305	Metapelite/-psammite	58
	Kai2	1009	Metapelite/-psammite	50
	Kai3	737	Metapelite/-psammite	40
	Kai4	407	Metapelite/-psammite	28
Riniken	Rin1	1797	Breccia	83
	Rin2	1628	Breccia	78
	Rin3	1381	Breccia	70
	Rin4	1181	Sandstone	65
	Rin5	992	Sandstone	58
Leuggern	Leu1	1684	Two-mica-granite	70
	Leu2	1249	Metapelite/-psammite	55
	Leu3	916	Metapelite/-psammite	42
	Leu4	567	Metapelite/-psammite	30
Siblingen	Sib1	1519	Cordierite-biotite-granite	58
	Sib2	1220	Cordierite-two-mica-granite	49
	Sib3	930	Cordierite-biotite granite	37
	Sib4	639	Cordierite-biotite-granite	32

2002) and by the deformation of Pliocene fluvial gravels (Giamboni et al. 2004a) and Quaternary terraces (Giamboni et al. 2004b).

3. Methodology

3.1 Basics of FT analysis

FT analysis of zircon and apatite is a powerful tool in assessing the thermal history of rocks in the temperature range of ~ 60–300 °C, which characterises the upper few kilometres of the crust. It is based on the spontaneous nuclear fission of ^{238}U (Price & Walker 1962a, 1962b) inducing a damage trail in the crystal, i.e. the latent fission tracks. After revelation of the latent tracks by chemical etching of polished grain-internal surfaces, the spontaneous track density may be counted. The FT age is calculated from the ratio of the spontaneous track density N_s observed on the polished surface and the induced track density N_i measured in an external detector after an irradiation procedure. A detailed overview of the principles of FT dating was provided, for instance, by Wagner & Van den Haute (1992), Gallagher et al. (1998) and Gleadow & Brown (2000).

The linear damage trails are stable over geological time only at relatively low temperatures and they become shorter by a process known as annealing at elevated temperatures. This reduction in length depends on the maximum temperature that each individual FT has experienced after its formation. Apart from other factors (e.g. chemistry, α-damage) temperature and time are clearly the most important factors for annealing of fission tracks. Since new tracks are continuously produced due to spontaneous decay, characteristic track length distributions can result depending on the thermal history to which the mineral grain has been exposed. Thus, the process of annealing is the key to the study of thermal histories by FT analysis. Modelling of FT annealing allows constraining the thermal history of rocks by matching observed and modelled FT parameters (FT age and length distribution).

3.2 Analytical details

Seventeen samples from drill cores of four Nagra boreholes were collected (Fig. 2, Table 1). After crushing and sieving, mineral separation was performed using conventional magnetic and heavy liquid techniques. Apatites were mounted in epoxy resin, zircons in PFA® Teflon. A sequence of grinding and polishing steps was carried out on the mounts in order to reveal grain-internal surfaces. Apatites were etched for 40 sec in HNO_3 (6.5 %) at room temperature, zircons for 4 to 14 h in a KOH-NaOH eutectic melt at 220 °C. Thermal neutron irradiation was carried out at the Australian Nuclear Science and Technology Organisation (ANSTO) facility, Lucas Heights, Australia. External mica detectors were etched for 40 min in HF (40 %) at room temperature. Tracks were counted and measured under an optical microscope with the aid of a computer driven stage (Dumitru 1993). Magnification used was 1600× using a dry objective for apatite FT analysis (track counting and confined track length measuring) and 2500× using an oil immersion objective for zircon FT analysis. FT ages were calculated according to the external detector method (Naeser 1976; Gleadow 1981) and the zeta approach (Hurford & Green 1982, 1983) with a zeta value of 345.69 ± 8.75 (Durango, CN5) for apatite and 113.49 ± 1.80 (Fish Canyon Tuff, CN1) for zircon. FT age and error calculation as well as the generation of the graphical representation were
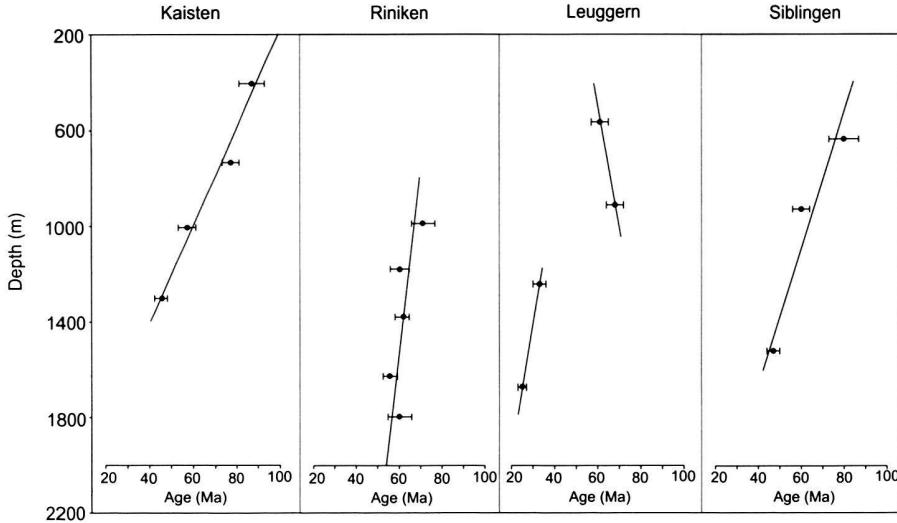
Fig. 3. Apatite FT central age (with 1σ error) versus depth graphs of the investigated Nagra boreholes. The Leuggern samples are splitted in two separate age groups as indicated by their thermal modelling results.
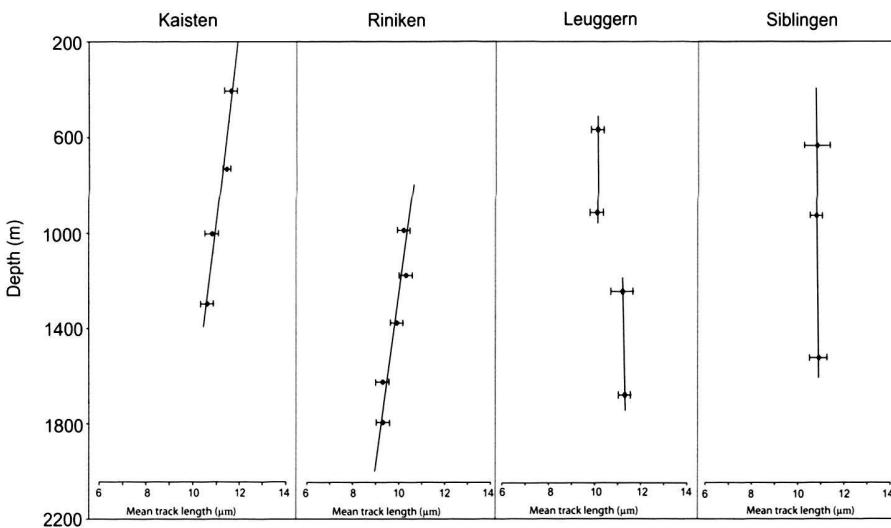

Fig. 4. Mean track length versus depth graphs of the investigated Nagra boreholes.

performed by the computer program Trackkey (Dunkl 2002). All FT ages are central ages (Galbraith & Laslett 1993) and errors are quoted as ± 1σ.

Thermal modelling of the apatite FT data was performed using the computer program AFTSolve (Ketcham et al. 2000) and the algorithm of Laslett et al. (1987), which is a numerical characterization of apatite FT annealing as a function of time and temperature. It is assumed that there is no significant difference in the annealing behaviour between the apatites of this study and the Durango apatite on which the algorithm of Laslett et al. (1987) is based. In this study an inverse modelling approach was carried out: a set of t-T paths was assessed that is consistent with the measured FT data in apatite and other geological constraints. The modelling process includes the generation of a large number of potential t-T paths and the statistical evaluation of the quality of the fit between predicted (based on

each t-T path generated) and the measured FT data in apatite (for details see Ketcham et al. 2000). As a result two regions outline all "acceptable" fits (light grey regions) with a Kolmogorov-Smirnov probability of 0.05 or more and "good" fits (dark grey regions) with a Kolmogorov-Smirnov probability of 0.5 or more (Ketcham et al., 2000). The best-fit t-T path is also included in each diagram. However, it has to be noted that the envelopes do not encompass t-T fields in which *all* t-T paths pass the corresponding statistical tests.

4. Analytical results

Seventeen core samples yielded fourteen zircon and sixteen apatite ages. Both zircon and apatite FT central ages are very similar in all boreholes, zircon FT central ages in total varying between 185 ± 16 Ma and 287 ± 21 Ma (Fig. 2, Table 2) and ap-

Table 2. Zircon FT age data from four boreholes (Nagra) in Northern Switzerland

Sample number	Depth (m)	No. of crystals counted	Spontaneous tracks ρ_s (N_s)	Induced tracks ρ_i (N_i)	$P(\chi^2)$ (%)	Dosimeter ρ_d(N_d)	Central age (Ma) ± 1σ
Kaisten							
Kai 1	1305	20	237 (1812)	21 (162)	54	3.94 (1497)	245 ± 22
Kai 4	407	20	210 (1636)	19 (152)	85	3.88 (1474)	233 ± 21
Riniken							
Rin 1	1797	20	333 (2985)	27 (242)	85	4.19 (1592)	287 ± 21
Rin 2	1628	20	350 (4652)	34 (453)	29	4.15 (1577)	238 ± 14
Rin 3	1381	20	328 (2329)	31 (217)	80	4.12 (1566)	246 ± 19
Rin 4	1181	20	262 (2453)	21 (198)	88	4.08 (1550)	281 ± 22
Rin 5	992	20	307 (1672)	26 (141)	99	4.05 (1539)	267 ± 25
Leuggern							
Leu 1	1684	20	324 (2177)	32 (216)	84	4.37 (1660)	245 ± 19
Leu 3	916	20	224 (1506)	20 (137)	98	4.31 (1638)	264 ± 25
Leu 4	567	20	246 (1225)	24 (119)	99	4.26 (1619)	244 ± 25
Siblingen							
Sib 1	1519	20	361 (2103)	35 (203)	<1	4.01 (1524)	225 ± 24
Sib 2	1220	20	319 (1066)	35 (118)	99	3.99 (1516)	201 ± 20
Sib 3	930	20	318 (1451)	29 (134)	99	3.97 (1509)	240 ± 23
Sib 4	639	20	347 (1711)	41 (204)	24	3.96 (1505)	185 ± 16

Track densities (ρ) are in 10^5 tracks/cm2, number of tracks counted (N) shown in brackets.
Analyses by external detector method using 0.5 for the $4\pi/2\pi$ geometry correction factor.
Ages calculated as central ages according to Galbraith and Laslett (1993) using dosimeter glass CN1 with ξ_{CN1} = 113.49 ± 1.80 (Z. Timar-Geng).
$P(\chi^2)$ is the probability of obtaining χ^2 value for v degrees of freedom where v = number of crystals - 1.

atite FT central ages varying between 25 ± 2 Ma and 87 ± 6 Ma (Fig. 2, Table 3) with a trend of decreasing ages with depth (Fig. 3). Mean track lengths exhibit a similar decreasing tendency with increasing borehole depth (Fig. 4).

4.1 Kaisten

In the Kaisten borehole metapsammitic layers of the crystalline basement beneath 172 m sediments of the Permian trough shoulder were sampled from a depth range between 407 m and 1306 m and present-day temperatures of 28° to 58 °C (Table 1).

Two samples yielded similar zircon FT ages of 233 ± 21 Ma and 245 ± 22 Ma from the top and the bottom of the entire sampled depth range (Figs. 2, 5). Radial plots (Galbraith 1988, 1990) of both zircon samples display relatively broad single-grain age distributions from ~400 to ~130 Ma. This high scatter of single-grain ages can be explained with normal Poissonian variation as revealed by the applied χ^2 statistics (Table 2), i.e. $P(\chi^2)$ values >5% indicate that all grains analysed for individual samples may be derived from a single age population (Green 1981). However, Timar-Geng et al. (2004) showed that high standard errors of single-grain age estimates and the low number of counted grains can render the χ^2-approach unsuitable for detection of any extra-Poissonian variation due to, for instance, different annealing kinetics of the individual grains.

Apatite FT ages vary from 45 ± 3 Ma at the bottom to 87 ± 6 Ma at the top of the sampled depth range with a clear younging trend toward depth (Figs. 2, 5). Single-grain ages scatter between ~140 Ma and ~30 Ma, the two youngest samples (Kai1 and Kai2) revealing very low $P(\chi^2)$ values (Table 3), which is an indication of extra-Poissonian variation in the spread of these ages. Confined mean track lengths ranging between 10.6 µm and 11.6 µm together with standard deviations all greater than 1.4 µm (Fig. 5) clearly show substantial partial annealing of all samples. In addition, decreasing apatite FT ages correlate with decreasing track lengths.

4.2 Riniken

Riniken is the only borehole of this study that penetrates the deep Permo-Carboniferous trough of northern Switzerland (Nagra 1990). Permian breccias and sandstones were sampled from a depth range between 992 m and 1797 m (Table 1).

Zircon FT central ages scatter between 238 ± 14 Ma and 287 ± 21 Ma (Figs. 2, 6). The large spread in single-grain ages (~460 Ma to ~ 130 Ma) with a significant proportion of pre-depositional single-grain ages indicate that none of the samples experienced palaeotemperatures critical for complete annealing of fission tracks in zircon, i.e. ~330 °C (Tagami & Shimada 1996; Tagami et al. 1998) since deposition. Thus, these samples exhibit a strong inherited signal from the source region.

Table 3. Apatite FT age data from four boreholes (Nagra) in Northern Switzerland

Sample number	Depth (m)	No. of crystals counted	Spontaneous tracks ρ_s (N_s)	Induced tracks ρ_i (N_i)	$P(\chi^2)$ (%)	Dosimeter $\rho_d(N_d)$	Central age (Ma) ± 1σ
Kaisten							
Kai 1	1305	20	8 (620)	33 (2590)	<1	10.77 (4092)	45 ± 3
Kai 2	1009	20	15 (1040)	49 (3377)	<1	10.48 (3982)	57 ± 4
Kai 3	737	20	22 (1404)	50 (3227)	12	10.19 (3872)	77 ± 4
Kai 4	407	20	5 (463)	10 (910)	35	9.91 (3766)	87 ± 6
Riniken							
Rin 1	1797	20	13 (864)	48 (3263)	<1	13.92 (5290)	62 ± 5
Rin 2	1628	20	20 (2503)	73 (9358)	<1	13.06 (4963)	58 ± 3
Rin 3	1381	20	18 (1504)	63 (5214)	2.13	12.77 (4853)	63 ± 3
Rin 4	1181	20	12 (1080)	41 (3663)	<1	12.20 (4636)	62 ± 4
Rin 5	992	20	18 (1324)	49 (3706)	<1	11.34 (4309)	72 ± 5
Leuggern							
Leu 1	1684	20	8 (425)	66 (3463)	<1	11.24 (4271)	25 ± 2
Leu 2	1249	20	4 (141)	21 (857)	36	11.47 (4359)	33 ± 3
Leu 3	916	20	14 (727)	33 (1681)	65	9.17 (3485)	68 ± 4
Leu 4	567	20	8 (719)	20 (1895)	7	9.35 (3553)	61 ± 4
Siblingen							
Sib 1	1519	20	14 (542)	46 (1800)	39	9.05 (3439)	47 ± 3
Sib 3	930	20	21 (657)	51 (1578)	<1	8.48 (3222)	60 ± 4
Sib 4	639	20	29 (531)	51 (926)	<1	8.19 (3112)	80 ± 7

Track densities (ρ) are in 10^5 tracks/cm², number of tracks counted (N) shown in brackets.
Analyses by external detector method using 0.5 for the $4\pi/2\pi$ geometry correction factor.
Ages calculated as central ages according to Galbraith and Laslett (1993) using dosimeter glass CN5 with ξ_{CN5} = 345.69 ± 8.75 (Z. Timar-Geng).
$P(\chi^2)$ is the probability of obtaining χ^2 value for v degrees of freedom where v = number of crystals - 1.

Apatite FT central ages range between 58 ± 3 Ma and 72 ± 5 Ma (Figs. 2, 6) with only a weak tendency of decreasing ages with depth. Radial plots (Fig. 6) display a large spread in the single-grain ages, varying between ~160 Ma and ~25 Ma. In all of the samples multiple age populations are present as revealed by the χ^2 statistics (Table 3). Substantial annealing is indicated by short confined mean track lengths of 9.3 μm to 10.2 μm and standard deviations greater than 1.7 μm.

4.3 Leuggern

A two-mica granite at the bottom and paragneisses at shallower depths were sampled in the Leuggern borehole between 567 m and 1684 m depth (Table 1).

Three samples yield uniform zircon FT central ages of 245 ± 19 Ma at the bottom, 244 ± 25 Ma at the top and 264 ± 25 Ma in-between (Figs. 2, 7). Single-grain ages range between ~450 Ma and ~ 140 Ma with no statistical indication for extra-Poissonian variation (Table 2).

Apatite FT central ages vary between 25 ± 2 Ma and 68 ± 4 Ma with a striking jump in the FT ages between Leu2 and Leu3 (Fig. 7). This feature is also visible in the confined mean track lengths, the two younger samples (Leu1 and Leu2) having longer mean track lengths (11.3 μm and 11.2 μm) than the older ones (Leu3 and Leu4 with mean track lengths of 10.1 μm), but *not* in the zircon FT central ages. Standard devia-

tions are greater than 1.8 μm. A distinction in two age groups is also reflected in the single-grain age distributions. Radial plots of the two younger samples (Leu1 and Leu2) display a single-grain age variation between ~60 Ma and ~10 Ma, while the older ones (Leu3 and Leu4) reveal a distribution of significantly older single-grain-ages from ~120 Ma to ~ 40 Ma (Fig. 7). Only Leu1 reveals a statistically founded indication for multiple age populations (Table 3).

4.4 Siblingen

Cordierite-biotite- and cordierite-two-mica-granites were sampled in the Siblingen borehole between 639 m and 1519 m depth (Table 1).

Zircon FT central ages scatter between 185 ± 16 Ma and 240 ± 23 Ma (Figs. 2, 8). There is a large spread in single-grain ages (~470 Ma to ~100 Ma), but only the sample at the bottom of the borehole (Sib1) has a $P(\chi^2)$ value lower than 5% (Table 2), thus indicating extra-Poissonian variation. Such isolated variation could be due to different annealing kinetics of the individual grains.

Apatite FT central ages range between 47 ± 3 Ma and 80 ± 7 Ma (Figs. 2, 8) with a clear tendency of decreasing ages with depth. Contrary to the zircon FT results Sib1 is the only sample showing no extra-Poissonian variation with a relatively narrow range of single-grain ages (~80 Ma to ~30 Ma). Radial
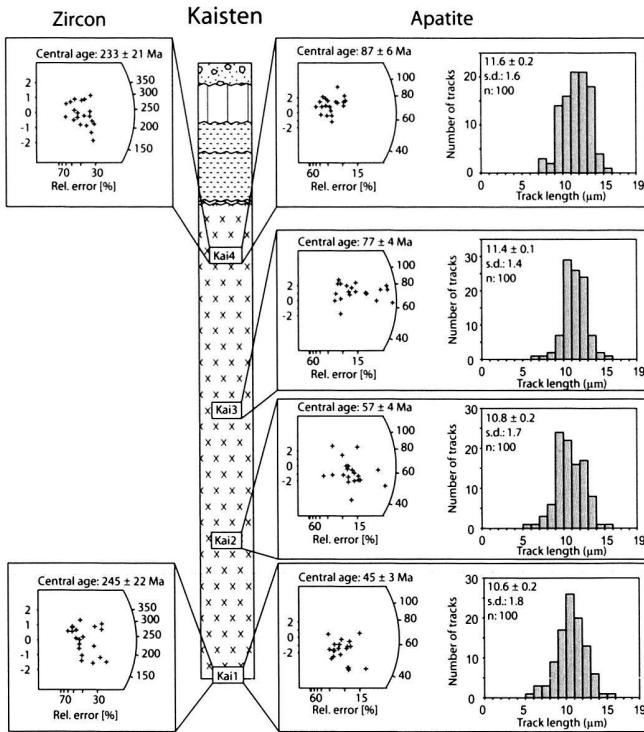
Fig. 5. Kaisten borehole: radial plots and track length distributions. For data, see Tab. 2 (zircon) and Tab. 3 (apatite). For geological unit patterns, see Fig. 2.


Fig. 6. Riniken borehole: radial plots and track length distributions. For data, see Tab. 2 (zircon) and Tab. 3 (apatite). For geological unit patterns, see Fig. 2.

plots of the other samples reveal single-grain ages up to ~130 Ma (Fig. 8). Confined mean track length in Sib3 (the only sample with the standard amount of 100 measurable confined horizontal tracks) is 10.8 ± 1.9 μm.

5. Thermal modelling

5.1 Modelling strategy

The low-temperature thermal history of northern Switzerland was derived using the following modelling strategy: Initial model runs were performed with only a few constraints on the time-temperature (t-T) path of each sample. The time for the first constraint was chosen on the base of the zircon FT age of the same sample and the oldest apatite single-grain age. This date should be somewhat older than the FT age of the oldest and thus most resistant apatite grains to allow for age reduction by partial annealing (Ketcham et al. 2000). The temperature for the first constraint was set at ~130 °C ensuring that there are no apatite fission tracks present as an initial condition. The last time constraint was set at the temperature at which the sample was collected (Nagra 1990, 1991a, 1991b, 1993). Modelled t-T paths were defined to be non-monotonic. This configuration is aimed at finding solutions by the program, particularly any possible heating events and their timing. This first model runs also constrain the time of cooling of the

sample below the track retention temperature, which can be used as a new constraint for following model runs.

In a next step, the new initial constraint and additional intermediate constraints (Table 4) were used to better evaluate individual heating and cooling events. Thereby model runs were progressively refined by forcing restrictions on the t-T paths as suggested by successive modelling results using additional nodal points in the region of assumed thermal events. Several possibilities regarding the timing of such a heating event were tested in an effort to find the temperature peak most consistent with the measured data. In a final step a narrower search was carried out using monotonic t-T paths between two user-defined constraints. This option potentially reduces the full extent of the envelope of statistically acceptable solutions, but simultaneously disables the modelled t-T paths to bounce up and down in a geologically inappropriate fashion (Ketcham et al. 2000). An example of the modelling procedure up to the "final" result is illustrated for sample Kai2 (Fig. 9).

5.2 Model results

5.2.1 Kaisten

Modelling of the apatite FT data from the Kaisten borehole samples (Fig. 10) indicates total track annealing since the be-
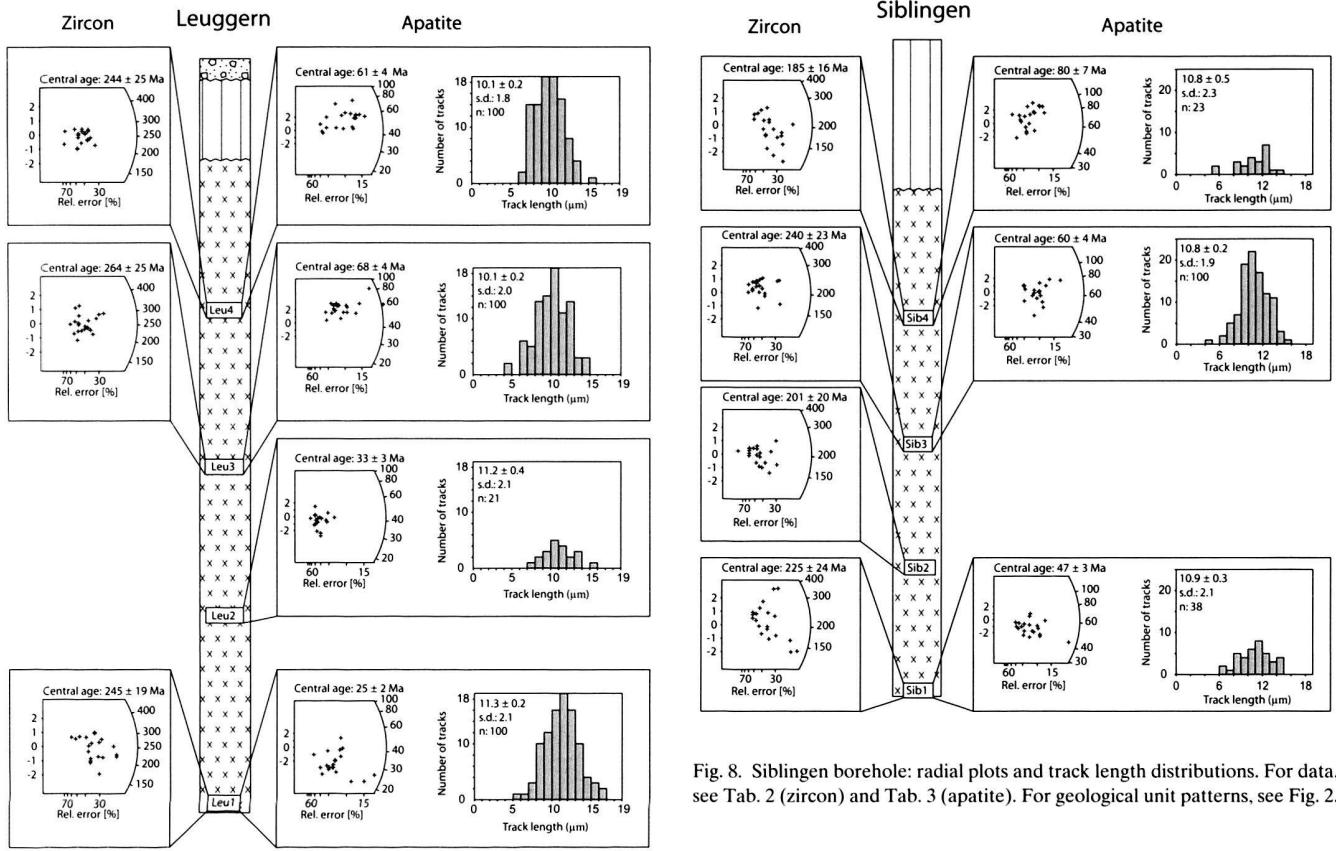
Fig. 7. Leuggern borehole: radial plots and track length distributions. For data, see Tab. 2 (zircon) and Tab. 3 (apatite). For geological unit patterns, see Fig. 2.

Fig. 8. Siblingen borehole: radial plots and track length distributions. For data, see Tab. 2 (zircon) and Tab. 3 (apatite). For geological unit patterns, see Fig. 2.

Table 4. Modelling details

| Samples	Constraints of final models (Ma, °C-°C)	Iterations	Nodal points
Kaisten			
Kai1	(0.0, 59-59)(11, 130-40)(30, 133-40)(35, 132-39)(40,130-40)(66, 130-40)(80, 129-129)	10,250	15
Kai2	(0.0, 51-51)(9.5, 129-31)(30, 128-34)(35, 129-33)(75, 130-41)(90, 130-130)	10,000	25
Kai3	(0.0, 40-40)(4.7, 100-40)(25, 113-41)(31, 100-21)(75, 100-21)(100, 132-132)	10,000	25
Kai4	(0.0, 29-29)(5.2, 126-30)(25, 126-31)(30, 125-30)(76, 126-30)(120, 130-130)	10,250	25
Riniken			
Rin1	(0.0, 84-84)(35, 128-84)(39, 128-30)(130, 106-30)(181, 130-130)	10,250	41
Rin2	(0.0, 78-78)(35, 132-60)(40, 119-20)(75, 117-21)(141, 131-131)	100,000	41
Rin3	(0.0, 70-70)(4.8, 130-86)(35, 130-66)(41, 128-23)(75, 127-26)(121, 130-130)	500,000	49
Rin4	(0.0, 65-65)(35, 122-26)(40, 102-20)(75, 133-21)(120, 132-132)	100,000	41
Rin5	(0.0, 59-59)(4.8, 120-78)(30, 111-71)(40, 129-24)(75, 129-23)(121, 131-131)	100,000	25
Leuggern			
Leu1	(0.0, 71-71)(40, 130-130)	10,000	33
Leu2	(0.0, 56-56)(51, 131-131)	10,000	33
Leu3	(0.0, 42-42)(10, 114-13)(35, 122-9)(40, 122-9)(75, 102-14)(121, 130-130)	112,183	49
Leu4	(0.0, 30-30)(10, 95-19)(36, 128-19)(40, 127-17)(90, 98-23)(121, 131-131)	10,000	49
Siblingen			
Sib1	(0.0, 59-59)(35, 123-25)(40, 103-26)(65, 130-25)(80, 129-129)	10,000	41
Sib2	(0.0, 37-37)(35, 129-40)(41, 108-20)(75, 117-25)(100, 130-130)	150,000	41
Sib3	(0.0, 33-33)(30, 128-20)(35, 98-16)(75, 129-21)(121, 130-130)	10,000	41

Fig. 9. Illustration of the modelling procedure (sample Kai2). From left to right: initial step with only a few constraints and non-monotonic t-T paths; intermediate step with more restrictions, as suggested by first model runs (e.g. initial constraint at 90 Ma) but still with non-monotonic t-T paths; "final" result with monotonic t-T paths between user-defined constraints.

ginning of the Mesozoic subsidence. Thus, the maximum palaeo-temperatures after post-Variscan peneplanation exceeded 120 °C. Oldest tracks preserved in the best-fit models vary from 75 Ma at the bottom of the sampled depth interval to 115 Ma at the top. This trend of increased track annealing with depth is consistent with the age data and can be interpreted in terms of increasing down-hole palaeo-temperatures. Measured and predicted parameters of the best-fit paths are in very good agreement, with age goodness-of-fit values of up to 0.98.

All four models (Fig. 10) display a two-phase cooling history since the samples cooled below the track retention temperature of ~120 °C. Moderate to rapid Cretaceous cooling through the apatite partial annealing zone (PAZ), i.e. through 120 °C to 60 °C, was followed by an Eo-Oligocene heating event and subsequent slow cooling to present-day temperatures. During the late cooling phase all samples remained within the PAZ until comparatively recent times.

5.2.2 Riniken

Best-fit models of the Riniken samples (Fig. 11) suggest that there was total annealing of fission tracks in Mesozoic times. Oldest tracks preserved in the best-fit models scatter between 113 Ma and 154 Ma. Evaluation of the statistical goodness-of-fit of modelled FT length distributions and ages to the measured data yields values between 0.63 and 0.99 (Fig. 11).

The modelled best-fit t-T paths are very similar for all samples. After Late Jurassic to Cretaceous cooling below the closure temperature of the apatite FT system a new heating phase started in the Late Eocene. After this heating event annealing temperatures persisted until recent times, which is also implied from the scarcity of very long tracks (Fig. 6).

5.2.3 Leuggern

The modelled t-T paths of the Leuggern borehole samples show two groups of markedly different shape (Fig. 12). The two upper samples (Leu3 and Leu4) experienced last resetting

of the apatite FT system in Mesozoic times. Best-fit models of the two lower samples (Leu1 and Leu2) indicate total annealing during the Eocene preserving oldest tracks with an age of 37 Ma (Leu1) and 48 Ma (Leu2). Preserved oldest tracks in the best-fit models of the two other samples are significantly older (118 Ma and 121 Ma). The statistical precision of the best-fit t-T paths is especially good for the two samples with short thermal histories (Leu1 and Leu2) with goodness-of-fit values >0.95. Somewhat lower but still "good" values were obtained for the two upper samples (Fig. 12).

Modelled t-T paths of both Leu3 and Leu4 display a common thermal history. Initial cooling below track retention temperatures in Cretaceous times and subsequent residence at moderate temperatures were followed by a prominent heating event during the Eocene. After this heating episode the samples remained within the PAZ until almost recent times. Apatite FT data of the two other samples (Leu1 and Leu2) recorded only the last cooling phase since the Eocene (Fig. 12).

5.2.4 Siblingen

Best-fit models of the Siblingen borehole samples (Fig. 13) indicate total annealing of apatite fission tracks during the Cretaceous. Oldest tracks preserved in the best-fit models range from 74 Ma (bottom) to 115 Ma (top), displaying a trend of increased track annealing with depth. Excellent age goodness-of-fit values of up to 0.99 prove that measured FT data and predicted parameters of the best-fit paths are in very good agreement.

All three models (Fig. 13) exhibit very comparable thermal histories with two cooling phases separated by a distinct heating event. The first cooling phase started in Cretaceous times and is characterised by moderate to rapid cooling rates. This cooling phase is followed by a heating event during the Eocene and a subsequent slow cooling phase to present-day temperatures. During the last cooling phase annealing temperatures have been maintained until comparatively recent times.
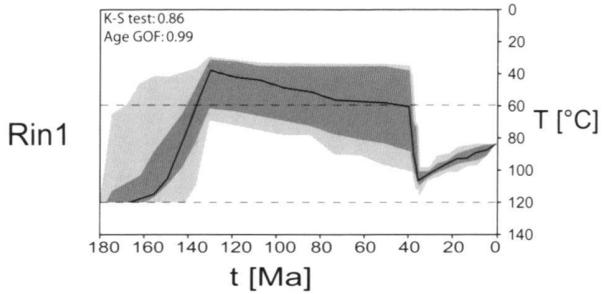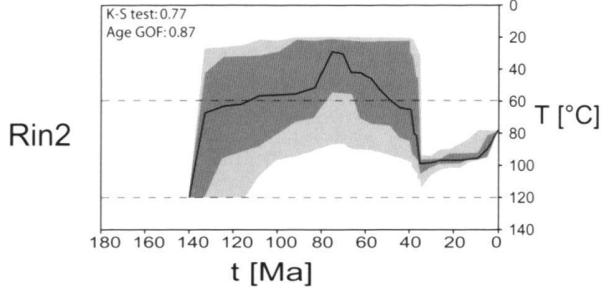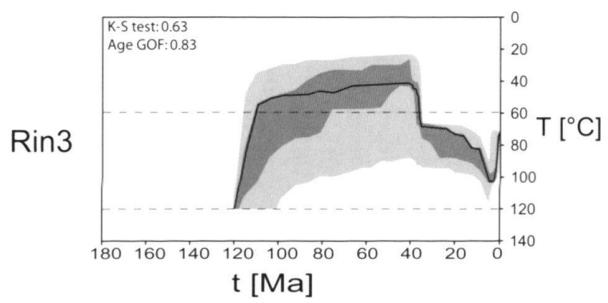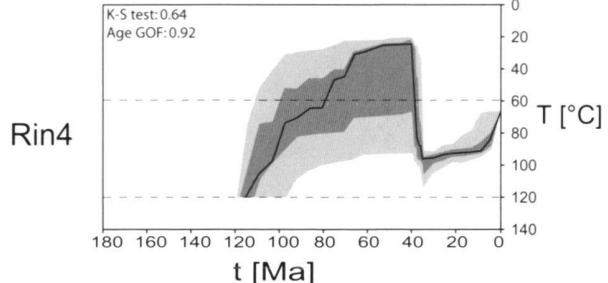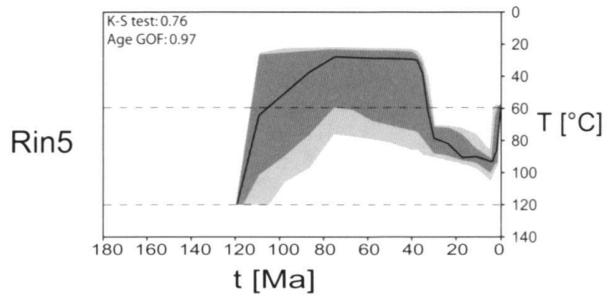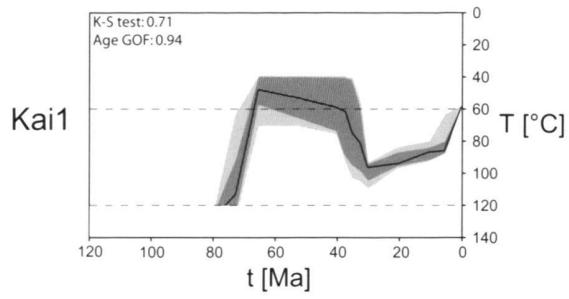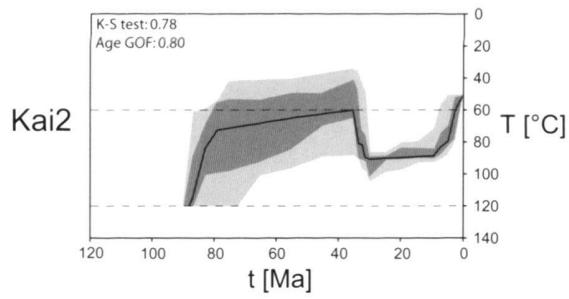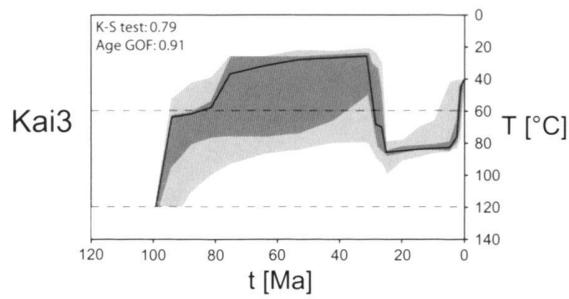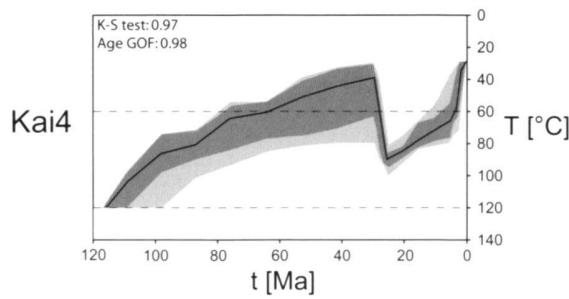
Fig. 10. Kaisten borehole: thermal modelling results. K-S test: Kolmogorov-Smirnov test evaluating the degree of fit between FT length distributions. Age GOF: FT age goodness-of-fit test. For details see Ketcham et al. (2000).


Fig. 11. Riniken borehole: thermal modelling results. For abbreviations, see Fig. 8.
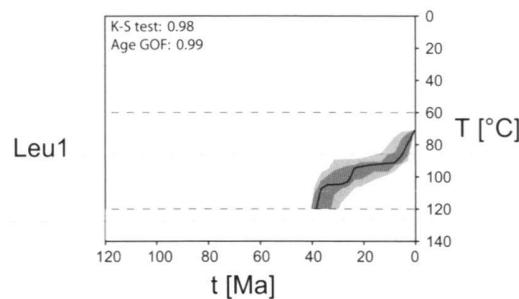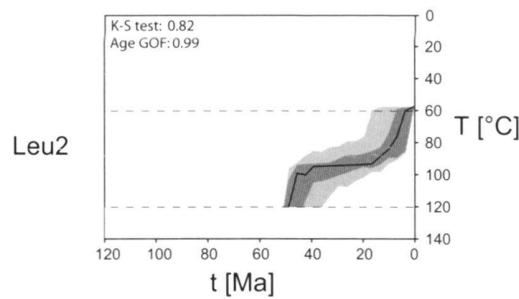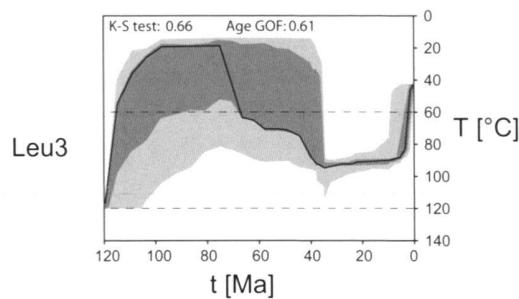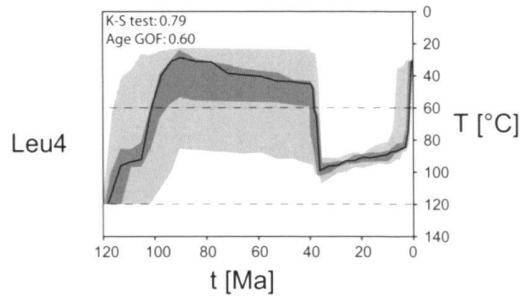
Fig. 12. Leuggern borehole: thermal modelling results. For abbreviations, see Fig. 8.
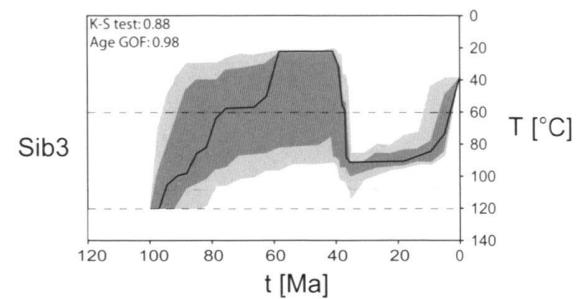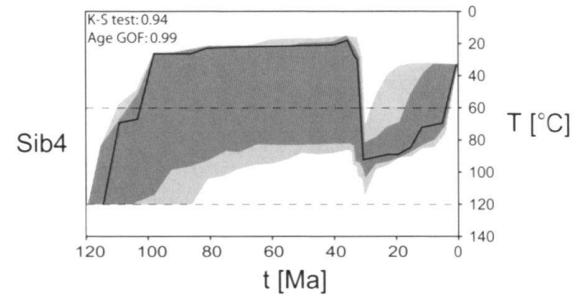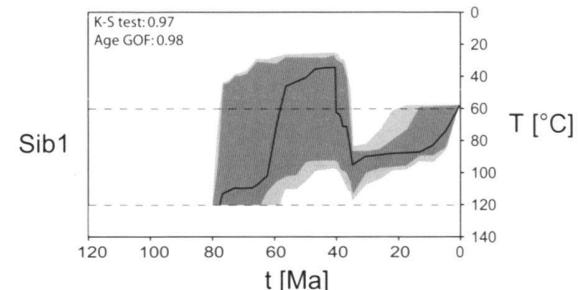
Fig. 13. Siblingen borehole: thermal modelling results. For abbreviations, see Fig. 8.

6. Discussion

The zircon FT ages indicate that in all boreholes the level of the crust sampled in northern Switzerland never experienced temperatures in excess of ~330 °C after the late Variscan consolidation of the crystalline basement, since total annealing of fission tracks in zircon is not observed. Zircon FT central ages and single-grain ages cluster at around 250 Ma and are substantially older than the central and single-grain ages from the nearby Black Forest (Fig. 14). The crystalline basement of northern Switzerland may be considered as the southern continuation of the internal zone of the Central European Variscides, now exposed in the Black Forest (e.g., Thury et al.

1994). The present-day outcrop level of the Black Forest approximately corresponds to the sampled depth range of the boreholes during Mesozoic subsidence. This can be stated because the Permo-Triassic paleosurface is partly preserved in the southern Black Forest (Paul 1955; Wimmenauer & Schreiner 1990). Primarily the Tertiary uplift of the Black Forest and the subsidence of the Alpine foreland, which was accompanied by reactivation of old fault zones in the study area (e.g., Müller et al. 2002), led to the current altitude difference between the two geographically neighbouring regions. Timar-Geng et al. (2004) interpreted the zircon FT data from the Black Forest in terms of a Jurassic heating event caused by regional-scale hydrothermal fluid migration. Obviously this thermal overprint is not observable from FT data in the borehole samples of northern Switzerland. Also, there is no other geological evidence for a main Jurassic hydrothermal phase in the crystalline basement of northern Switzerland. The youngest penetrative thermal event with a clear petrographic signature is a kaolinitic alteration and the formation of interconnected vugs in pre-existing structures with weakly constrained post-Permian ages (Mazurek et al. 1992) and authigenic illite formation in sandstones in the Jurassic (Schaltegger et al., 1995). Based on coalification and fission track data, Schegg & Leu (1998) estimated high palaeogeothermal gradients of 80–90 °C/km in northern Switzerland during the Late Palaeozoic. The zircon FT data of this study bear the signature of this regional thermal event, which also correlates with the rhyolitic volcanism known in the Black Forest. Common for both the Black Forest and the crystalline basement of northern Switzerland is the Cretaceous cooling below the zircon FT PAZ, i.e. below ~200 °C (e.g., Tagami & Shimada 1996; Tagami et al. 1998; see also discussion in Timar-Geng et al. 2004). This is inferred from the youngest single-grain age cluster dating the passage through the low-temperature boundary of the PAZ (Fügenschuh & Schmid 2003).

The apatite FT data document the low temperature (< ~120°C) thermal history of the region. The borehole samples mostly exhibit a trend of decreasing ages with depth (Fig. 3). This is a common feature in most geological settings and the shape of the age-depth graphs often reflects the thermal history of the rocks as they cooled through the PAZ (Gleadow & Brown 2000). Such age-depth profiles vary from nearly linear for high denudation rates to concave-upwards curves at low rates (Gleadow & Brown 2000). The age-depth trend of the Nagra borehole samples are approximated by a linear relationship, but a sound interpretation in terms of denudation rates is not recommended due to the measured track length distributions. In fact, thermal modelling of the FT data suggests a composite thermal history of the region with slow post-Eocene cooling and prolonged residence in the PAZ. The shape of the age-depth graph is, therefore, primarily controlled by the increase in temperature with depth and is not related to the denudation rate. There is a published apatite FT central age (160 ± 10 Ma; Mazurek et al. 2006) from the borehole Riniken from shallower depth, which is significantly older than the Riniken samples in this study. Most probably this sample did not experience total annealing but rather also contains inherited tracks.

Modelling of the apatite FT parameters provides a fairly clear picture about the low-temperature thermal history of the crystalline basement of northern Switzerland since Cretaceous times (Figs. 10–13). All t-T paths (with the exception of Leu1 and Leu2) exhibit the same general shape: moderate to rapid Cretaceous cooling through the PAZ is followed by Eocene heating in-between the PAZ and subsequent cooling to present-day temperatures. The second cooling phase is characterised by prolonged residence in the PAZ. This is also implied by strongly reduced mean track lengths (Fig. 4) and scarcity of long tracks. The two lower Leuggern borehole samples (Leu1 and Leu2) apparently experienced total track loss during the Eocene heating event. Therefore, only the last cooling phase is documented by the apatite FT parameters. It should be stated that in spite of the excellent statistical goodness-of-fit values, the modelled thermal histories need not be unique. A broad range of t-T paths may generate FT parameters that could lie behind the measured data (Ketcham et al. 2000). Furthermore, cooling phases prior to reheating are not well documented by FT data for those temperatures lying below the maximum temperature of the reheating event due to annealing of all pre-existing tracks (De Bruijne & Andriessen 2002). The maximum temperature of a reheating event is quite well determined by modelling studies (Gleadow & Brown 2000). However, due to statistical uncertainties in the evaluation of the best-fit paths, the reconstruction of palaeogeothermal gradients based on modelling results is not recommended.

Some previous apatite FT modelling studies (Nagra 2002; Mazurek et al. 2006) dealt with parts of the Swiss Molasse Basin, located only a few km further to the south of the area presented here. Combined with other methods, Mazurek et al. (2006) reconstructed a multi-stage burial history of the basin with two successive stages of heating, one in the Cretaceous and the other in the Miocene. They relate the first heating episode to Mesozoic burial *and* an increased heat flux of 85-100 mW/m^2 in the Early Cretaceous. The second heating stage was caused by maximum burial during the Miocene (Mazurek et al. 2006). The initial cooling phase of our samples into the PAZ roughly coincides with the first cooling stage after Cretaceous burial and heating presented by Mazurek et al. (2006). Thus, it appears that the same Mesozoic thermal event caused total track annealing in the sampled crustal level of the external parts of northern Switzerland, mostly north of the Permo-Carboniferous trough. However, Cretaceous heating of the internal parts of northern Switzerland postdates the peak of the Mesozoic hydrothermal alteration observed in the neighbouring Black Forest, even though a less clear record of hydrothermal activity in the crystalline basement throughout the Cretaceous is also available (see compilation by Wetzel et al. 2003). Thus, in the case of the samples presented here, increased heat flux values affect the experienced total annealing of apatite fission tracks rather than burial below Mesozoic sediments.
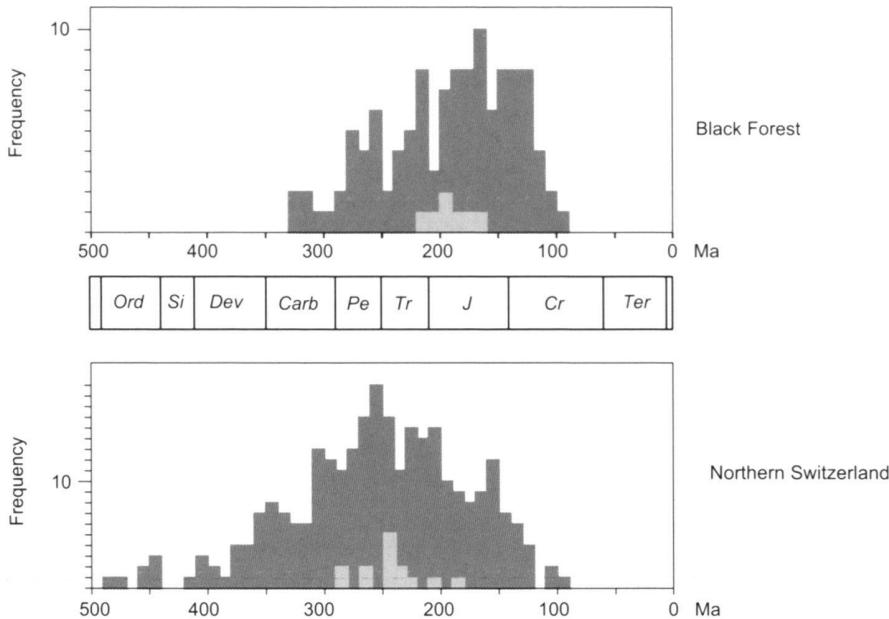
Fig. 14. Frequency distribution of central ages (light grey) and single-grain ages (dark grey) for the Black Forest (Timar-Geng et al., 2004) and northern Switzerland (this study).

The striking feature of the modelled t-T paths of the present study is a major heating event of mostly Middle to Late Eocene age, which clearly predates the second heating stage in the Molasse basin. However, this can be explained by the tectonically and palaeogeographically different settings of the two regions. The borehole samples of this study are situated outside or in a marginal position of the Molasse basin, whereas the previously analysed samples (Mazurek et al. 2006) experienced substantial burial due to the subsidence of the Alpine foreland from the Late Oligocene onwards. Consequently, the elevated temperatures during the Miocene burial phase (e.g., Mazurek et al. 2006) might have overprinted a possible Eocene thermal pulse in the more internal parts of the Molasse basin. The Eocene heating event recorded in the FT data of this study, in contrast, can be related to the initial rifting stage of the nearby Upper Rhine Graben in the foreland of the evolving Alps (e.g., Schumacher 2002). This initial rifting stage was controlled by the gradually increasing subduction resistance of the European lithosphere and the build-up of intraplate stresses (Dèzes et al. 2004), and accompanied by progressively increasing volcanic activity (e.g., Lippolt 1983; Keller et al. 2002). Reactivation of Permo-Carboniferous crustal-scale fault systems played a fundamental role during the initial, Late Eocene rifting phase of the Upper Rhine Graben (Schumacher 2002) and was also characteristic for the entire foreland of the Alps at this time (Dèzes et al. 2004). Thus, faults of the Permo-Carboniferous Trough of northern Switzerland could have also acted as major conduits for circulating hydrothermal fluids giving rise to the observed middle to Late Eocene thermal event in the crystalline basement of northern Switzerland.

A distinctly accelerated cooling towards the present-day temperature, displayed by almost all modelled t-T paths, appears to be an artefact of the Laslett et al. (1987) algorithm (e.g. Ketcham et al. 2000) and, hence, is not further discussed.

7. Conclusions

The low-temperature thermal history of the crystalline basement of northern Switzerland has been derived by FT analysis on 17 borehole samples. Inverse modelling techniques were used to provide quantitative constraints on time-temperature histories that are in agreement with the measured data.

Within the investigated borehole sections, maximum palaeotemperatures never exceeded ~330 °C since post-Variscan peneplanation. Zircon FT central and single-grain ages do not show evidence for a Jurassic hydrothermal event, as was observed in the nearby southern Black Forest (Timar-Geng et al. 2004, 2006). Instead, the zircon FT data bear the signature of elevated Late Palaeozoic palaeogeothermal gradients (Schegg & Leu 1998).

Modelling results suggest that moderate to rapid cooling of the samples through the apatite PAZ at the end of the Mesozoic was followed by a distinct thermal event during the Eocene and subsequent slow cooling to present-day temperatures. For the duration of the second cooling phase the samples remained within the PAZ until comparatively recent times or even until present.

The Eocene heating event coincides with the initial rifting phases of the neighbouring Upper Rhine Graben and associated volcanic activity. It is proposed that faults of the Permo-Carboniferous Trough of northern Switzerland could have acted as important pathways for migrating hydrothermal fluids inducing the observed middle to Late Eocene thermal anomaly in the crystalline basement of northern Switzerland.

REFERENCES

CEDERBOM, C.E., SINCLAIR, H.D., SCHLUNEGGER, F. & RAHN, M.K. 2004: Climate-induced rebound and exhumation of the European Alps. Geology 32, 709–712.

DE BRUIJNE, C.H. & ANDRIESSEN, P.A.M. 2002: Far field effects of Alpine plate tectonism in the Iberian microplate recorded by fault-related denudation in the Spanish Central System. Tectonophysics 349, 161–184.

DÈZES, P., SCHMID, S.M. & ZIEGLER, P.A. 2004: Evolution of the Alpine and Pyrenean orogens with their foreland lithosphere. Tectonophysics 389, 1–33.

DUDDY, I.R. 1994: The Otway Basin: thermal, structural, tectonic and hydrocarbon generation histories. In: FINLAYSON, D.M. (Ed.): NGMA/PESA Otway Basin Symposium, Extended Abstracts Record 1994, 35–42. Australian Geological Survey Organisation, Canberra.

DUMITRU, T.A. 1993: A new computer-automated microscope stage system for fission-track analysis. Nuclear Tracks and Radiation Measurements 21, 575–580.

DUNKL, I. 2002: Trackkey; a Windows program for calculation and graphical presentation of fission track data. Computers and Geosciences 28/1, 3–12.

EDEL, J.-B. 1997: Les réaimantations post-permiennes dans le bassin dévono-dinantien des Vosges méridionales; existence d'une phase de réaimantation au Lias, contemporaine de minéralisations d'ampleur régionale. Comptes Rendus de l'Academie des Sciences, Serie II. Sciences de la Terre et des Planètes 324/8, 617–624.

FÜGENSCHUH, B. & SCHMID, S.M. 2003: Late stages of deformation and exhumation of an orogen constrained by fission-track data: A case study in the Western Alps. Geol. Soc. Am. Bull. 115, 1425–1440.

GALBRAITH, R.F. 1988: Graphical display of estimates having differing standard errors. Technometrics 30, 271–281.

GALBRAITH, R.F. 1990: The radial plot: graphical assessment of spread in ages. Nuclear Tracks and Radiation Measurements 17, 207–214.

GALBRAITH, R.F. & LASLETT, G.M. 1993: Statistical models for mixed fission track ages. Nuclear Tracks Radiation Measurements 21, 459–70.

GALLAGHER, K., BROWN, R.W. & JOHNSON, C. 1998: Fission track analysis and its applications to geological problems. Ann. Rev. Earth Planet. Sci. 26, 519–572.

GIAMBONI, M., USTASZEWSKI, K., SCHMID, S.M., SCHUMACHER, M.E. & WETZEL, A. 2004a: Plio-Pleistocene transpressional reactivation of Paleozoic and Paleogene structures in the Rhine-Bresse transform zone (northern Switzerland and eastern France). Int. J. Earth Sci. 93, 207–223.

GIAMBONI, M., WETZEL, A, NIVIÈRE, B. & SCHUMACHER, M. 2004b: Plio-Pleistocene folding in the southern Rhinegraben recorded by the evolution of the drainage network (Sundgau area; northwestern Switzerland and France). Eclogae geol. Helv. 97, 17–31.

GLEADOW, A.J.W. 1981: Fission track dating: what are the real alternatives. Nucl. Tracks 5, 3–14.

GLEADOW, A.J.W. & BROWN, R.W. 2000: Fission-track thermochronology and the long-term denudational response to tectonics. In: Summerfield, M.A. (Ed.): Geomorphology and Global Tectonics. John Wiley & Sons, Chichester, United Kingdom, 57–76.

GLEADOW, A.J.W., DUDDY, I.R. & LOVERING, J.F. 1983: Fission track analysis: a new tool for the evaluation of thermal histories and hydrocarbon potential. Aust. Pet. Explor. Assoc. J. 23, 93–102.

GREEN, P.F. 1981: A new look at statistics in fission track dating. Nuclear Tracks and Radiation Measurements 5, 77–86.

GREEN, P.F., DUDDY, I.R., GLEADOW, A.J.W. & LOVERING, J.F. 1989: Apatite fission-track analysis as a paleotemperature indicator for hydrocarbon exploration. In: Naeser, N.D., McCulloh, T.H. (Eds.), Thermal History of Sedimentary Basins: Methods and Case Histories. Springer-Verlag, Berlin, 181–195.

GREEN, P.F., THOMSON, K. & HUDSON, J.D. 2001: Recognition of tectonic events in undeformed regions; contrasting results from the Midland Platform and East Midlands Shelf, central England. J. Geol. Soc. London 158, 59–73.

HOUSE, M.A., KOHN, B.P., FARLEY, K.A. & RAZA, A. 2002: Evaluating thermal history models for the Otway Basin, southeastern Australia, using (U-Th)/He and fission-track data from borehole apatites. Tectonophysics 349, 277–295.

HURFORD, A.J. & GREEN, P.F. 1982: A users' guide to fission track dating calibration. Earth Planet. Sci. Lett. 59/2, 343–354.

HURFORD, A.J. & GREEN, P.F. 1983: The zeta age calibration of fission-track dating. Chem. Geol. 41/4, 285–317.

KELLER, J., KRAML, M. & HENJES-KUNST, F. 2002: $^{40}Ar/^{39}Ar$ single crystal dating of early volcanism in the Upper Rhine Graben and tectonic implications. Schweiz. Mineral. Petrogr. Mitt. 82, 121–130.

KETCHAM, R., DONELICK, R. & DONELICK, M. 2000: AFTSolve: a program for multi-kinetic modelling of apatite fission track data. Geol. Mater. Res. 2/1, 1–18.

LASLETT, G., GREEN, P., DUDDY, I. & GLEADOW, A. 1987: Thermal annealing of fission tracks in apatite. Chem. Geol. 65, 1–13.

LIPPOLT, H.J. 1983: Distribution of volcanic activity in space and time. In: Fuchs, K., von Gehlen, K., Mälzer, M., Murawski, H. and Semmel, A. (Eds.), Plateau Uplift, The Rhenish Shield – A Case History. Springer-Verlag, Berlin, 112–120.

MAZUREK, M., MEYER, J. & PETERS, T. 1992: The crystalline basement of Northern Switzerland. Eclogae geol. Helv. 85/3, 767–769.

MAZUREK, M., HURFORD, A.J. & LEU, W. 2006: Unravelling the multi-stage burial history of the Swiss Molasse Basin: integration of apatite fission track, vitrinite reflectance and biomarker isomerisation analysis. Basin Research 18, 27–50.

MURAKAMI, M., TAGAMI, T. & HASEBE, N. 2002: Ancient thermal anomaly of an active fault system; zircon fission-track evidence from Nojima GSJ 750 m borehole samples. Geophys. Res. Lett. 29, 23.

MÜLLER, W.H., NAEF, H. & GRAF, H.R. 2002: Geologische Entwicklung der Nordschweiz, Neotektonik und Langzeitszenarien Zürcher Weinland. Nagra Tech. Ber. NTB 99–08, Nagra, Wettingen.

NAESER, C.W. 1976: Fission-track dating. Open-File Rep. – U. S. Geol. Surv. 76–190.

NAESER, C.W., McKEE, E.H., JOHNSON, N.M. & MacFADDEN, B.J. 1987: Confirmation of a late Oligocene-early Miocene age of the Deseadan Salla beds of Bolivia. J. Geol. 95, 825–828.

NAGRA 1990: Sondierbohrung Riniken. Untersuchungsbericht. Beiträge zur Geologie der Schweiz. Geotechnische Serie 74.

NAGRA 1991a: Sondierbohrung Leuggern. Untersuchungsbericht. Beiträge zur Geologie der Schweiz. Geotechnische Serie 75.

NAGRA 1991b: Sondierbohrung Kaisten. Untersuchungsbericht. Beiträge zur Geologie der Schweiz. Geotechnische Serie 83.

NAGRA 1993: Sondierbohrung Siblingen. Untersuchungsbericht. Beiträge zur Geologie der Schweiz. Geotechnische Serie 86.

NAGRA 2002: Projekt Opalinuston-Synthese der geowissenschaftlichen Untersuchungs-ergebnisse. Nagra Technical Report NTB 02–03, Nagra, Wettingen, Switzerland.

PAUL, W. 1955: Zur Morphogenese des Schwarzwaldes (I). Jahresheft geol. Landesamt Baden-Württ. 1, 395–427.

PRICE, P.B. & WALKER, R.M. 1962a: A new detector for heavy particle studies. Phys. Lett. 3, 113–115.

PRICE, P.B. & WALKER, R.M. 1962b: Observations of charged-particle tracks in solids. J. Appl. Phys. 33, 3400–3406.

SCHALTEGGER, U., ZWINGMANN, H., CLAUER, N., LARQUE, P. & STILLE, P. 1995: K–Ar dating of a Mesozoic hydrothermal activity in Carboniferous to Triassic clay minerals of northern Switzerland. Schweiz. Mineral. Petrogr. Mitt. 75, 163–176.

SCHEGG, R. & LEU, W. 1998: Analysis of erosion events and palaeogeothermal gradients in the North Alpine Foreland Basin of Switzerland. In: S.J. Düppenbecker and J.E. Iliffe (eds.): Basin Modelling: Practice and Progress. Geol. Soc. Spec. Publ. 141, 137–155.

SCHUMACHER, M.E. 2002: Upper Rhine Graben: Role of preexisting structures during rift evolution. Tectonics 21/1, 6, 1–17.

TAGAMI, T. & SHIMADA, C. 1996: Natural long-term annealing of the zircon fission track system around a granitic pluton. J. Geophys. Res. 101/B4, 8245–8255.

TAGAMI, T., GALBRAITH, R.F., YAMADA, R. & LASLETT, G.M. 1998: Revised annealing kinetics of fission tracks in zircon and geological implications. In: P. Van den Haute and F. De Corte (eds.): Advances in Fission Track Geochronology, Kluwer Academic Publishers, Dordrecht, 99–112.

THURY, M., GAUTSCHI, A., MAZUREK, M., MÜLLER, W.H., NAEF, H., PEARSON, F.J., VOMVORIS, S. & WILSON, W. 1994: Geology and Hydrology of the Crystalline Basement of Northern Switzerland. Nagra Tech. Ber. NTB 93–01, Nagra, Wettingen.

TIMAR-GENG, Z., FÜGENSCHUH, B., SCHALTEGGER, U. & WETZEL, A. 2004: The impact of the Jurassic hydrothermal activity on zircon fission track data from the southern Upper Rhine Graben area. Schweiz. Mineral. Petrogr. Mitt. 84, 257–269.

TIMAR-GENG, Z., FÜGENSCHUH, B., WETZEL, A. & DRESMANN, H. 2006: Low-temperature thermochronology of the flanks of the southern Upper Rhine Graben. Int. J. Earth Sci. 95, 685–702

TINGATE, P.R. & DUDDY, I.R. 2002: The thermal history of the eastern Officer Basin (South Australia): evidence from apatite fission track analysis and organic maturity data. Tectonophysics 349, 251–275.

WAGNER, G.A. & VAN DEN HAUTE, P. 1992: Fission track dating. Kluwer, Dordrecht, 285pp.

WETZEL, A., ALLENBACH, R. & ALLIA, V. 2003: Reactivated basement structures affecting the sedimentary facies in a tectonically "quiescent" epicontinental basin: an example from NW Switzerland. Sedimentary Geology 157/1–2, 153–172.

WIMMENAUER, W. & SCHREINER, A. 1990: Erläuterungen zu Blatt 8114, Feldberg. Geol. Karte Baden-Württ. 1:25 000, Stuttgart, 134 pp.

ZIEGLER, P.A. 1990: Geological Atlas of Western and Central Europe. Shell Internationale Petroleum Maatschappij – Geological Society Publishing House, 239 pp.